Enhanced biodegradation of polylactic acid and cellulose acetate nanocomposites in wastewater: Effect of TiO2 and β-cyclodextrin

Leire Goñi-Ciaurriz
University of Navarra
Adrián Durán
University of Navarra
Francisco J Peñas
University of Navarra
Itziar Vélaz (itzvelaz@unav.es)
University of Navarra

Research Article

Keywords: Biodegradation, TiO2 nanoparticles, β-cyclodextrin, Polylactic acid, Cellulose acetate, Nanocomposites

Posted Date: September 20th, 2022

DOI: https://doi.org/10.21203/rs.3.rs-2064652/v1

Abstract

Currently, there is a global concern about the environmental problems related to plastic wastes. Cellulose acetate (CA) and polylactic acid (PLA) are the most frequently used biopolymers in the food packaging industry. In this work, TiO_2 nanoparticles and β-cyclodextrin (βCD) have been incorporated into nanocomposite films made of PLA and CA and then evaluated under biodegradation assays in wastewater to assess the effects of both additives on the biodegradability of films. TiO_2 nanoparticles clearly enhanced the biodegradability of CA and PLA; PLA-TiO_2 nanocomposites disappeared after 60 days, whereas plain PLA remained present after 100 days. The presence of the additives provided an exponential growth to BOD profiles. FTIR spectra showed a much faster deacetylation of CA for the nanocomposites than for the bare CA, and XRD diffractograms showed that PLA nanocomposites became more amorphous than bare PLA. The thermal resistance of CA and PLA nanocomposites substantially decreased, while plain matrices remained fairly stable up to 60 days. SEM micrographs of CA and PLA nanocomposites presented voids and larger surface erosion than the plain matrices. βCD modification of TiO_2 nanoparticles seems to have a protective effect on the biodegradation of the polymers with respect to the unmodified TiO_2.

1. Introduction

Plastics have become essential in the current society due to their wide variety of applications. Thermoplastic polymers have advantages including high performance and ease processing, and thus they represent around 80% of the global plastic market [1]. However, most of them come from non-renewable fossil resources, and have raised serious environmental problems related to their manufacture and disposal through incineration and landfill processes [2, 3]. For this reason, many efforts are being made to replace petroleum-derived plastics with biodegradable materials, especially in short-term disposable packaging applications.

Biodegradable polymers have desirable functionalities while also contribute to sustainability [4, 5]. Polylactic acid (PLA) is a thermoplastic aliphatic polyester of lactic acid that can be easily obtained through the fermentation of renewable materials such as corn, potatoes, sugar or rice [6, 7]. PLA is considered as one of the most promising biopolymers for a variety of uses including packaging due to its interesting balance of properties (biocompatibility, transparency, low cost, easy processing and suitable barrier properties) [8, 9]. Moreover, its good mechanical strength is comparable to that of some conventional petroleum-derived polymers such as polystyrene (PS) or polyethylene terephthalate (PET) [10, 11]. Cellulose acetate (CA) is an alternative biopolymer with ample use, obtained from the chemical modification of cellulose with acetic anhydride and acetic acid. CA is biodegradable, capable of forming films and possesses high chemical and mechanical stability [12, 13].

Moreover, the development of next-generation packaging materials is becoming a research focus of the food industry. An interesting strategy to obtain improved packaging consist on incorporating metallic nanoparticles (NPs) during the films production. Titanium (IV) oxide (TiO_2) NPs have many advantages

such as photocatalytic properties, biocompatibility, high chemical stability and excellent antimicrobial activity against a wide variety of microorganisms [14]. Despite the current controversy surrounding the use of nanocompounds in food, TiO_2 NPs are approved to be used as safe additive by the American Food and Drug Administration (FDA) [15]. Moreover, several studies have demonstrated that the amount of TiO_2 NPs migrated from polymeric matrices into food simulants is minimal [16]. On the one hand, the incorporation of TiO_2 NPs as antimicrobial agents to the packages gives rise to the so-called active packaging. These novel materials provide greater protection against food spoilage and contribute to extend the shelf-life of the perishable food products [17]. On the other hand, they have been shown to enhance the mechanical, thermal and barrier properties of biodegradable polymers [18–20]. Finally, it has been reported that the inclusion of TiO_2 promotes photo- and thermo-degradation of biopolymeric materials, facilitating the plastic wastes disposal after their use [21–24]. However, the effect of NPs under biodegradation conditions is not yet well-known.

The modification of TiO_2 NPs with cyclodextrins (CDs) is a good way to increase their functionality [25]. Native CDs are cyclic oligosaccharides linked by α-1,4 glycosidic bonds and composed of 6 (αCD), 7 (βCD) or 8 (γCD) glucose units. They are natural compounds obtained by the enzymatic degradation of starch [26]. In terms of structure, CDs are truncated conical cylinders with a relatively apolar cavity and a polar outer surface, which allows them to form host-guest inclusion complexes with a variety of hydrophobic substances [27]. They have found applications in many fields, and currently their use in the food packaging industry is gaining attention. CDs can ensure a sustained release of active molecules such as food preservatives, while protecting them from heat and physical processes during the packages production [28]. Due to their biodegradable nature, when CDs are integrated with biodegradable polymer-binders, such as PLA or CA, the developed package will become completely eco-friendly [27, 29]. Furthermore, CDs may create weak-points in the packaging film where the degradation of composites would be promoted [30].

The idea that the biodegradability of plastics is the result of optimized laboratory conditions rather than spontaneously decompose in natural environments is controversial [31]. Therefore, it is important to study the biodegradation of materials in natural environments like sewages. Sewage sludge provides optimal conditions for the microorganisms to grow, since it contains organic carbon, nitrogen, phosphorous and other nutrients [32]. In this work active packaging film materials based on PLA or CA (7.5% wt/v) and containing 5% TiO_2 and 5% βCD-TiO_2 NPs (w/w) have been obtained (nanocomposites). Under the hypothesis that the inclusion of TiO_2 NPs and CDs into biopolymeric matrices will enhance their biodegradability, the performance of PLA and CA composites throughout long-term degradation assays in sewage sludge has been evaluated in terms of chemical-structure, thermal, morphological, and crystalline properties. The biochemical oxygen demand (BOD), which represents the amount of oxygen consumed by natural microorganisms to convert the obtained organic materials into microbial biomass [33, 34] has also been reported.

2. Materials And Methods

2.1. Materials

Titanium (IV) oxide nanoparticles (TiO_2 NPs 99.5% purity, 21 nm average size and $\rho = 4.26\ g \bullet cm^{-3}$) were provided by Sigma-Aldrich (St. Louis, MO, USA). β-Cyclodextrin (βCD 12.5% water content) was manufactured by Roquette (Laisa España S.A.). Acetone dry (≤ 0.01% water), N,N-dimethylformamide dry (DMF) and methanol (≤ 0.01% water) were supplied by Panreac Applichem. Hexamethylene diisocyanate (HMDI, 98%) was purchased from Fluka (Morris Planes, NJ, USA). Poly(L-Lactic acid) (PLA) was provided by Resinex Spain, S.L., and manufactured by Nature Works LLC (Blair, NE, USA) (Ref. code: PLA Polymer 7032D). Cellulose acetate (CA) was purchased from Rhodia.

2.2. Preparation of polymeric films

The detailed procedure including the obtention and further characterization of TiO_2 NPs functionalized with βCD was reported in a previous work [25]. In brief, hexamethylene diisocyanate was used as crosslinker between βCD and TiO_2, and the linkage was confirmed by Fourier transform infrared spectroscopy (FTIR) and thermogravimetric analysis (TGA) techniques after several washing and centrifugation steps. At the end of the process, the cyclodextrin content in the modified TiO_2 NPs was found to be 16%.

Using PLA and CA as biodegradable matrices, solution casting process was employed to prepare polymeric films with embedded modified and unmodified TiO_2 NPs [21]. Firstly, 3.75 g of PLA and 3.75 g of CA were completely dissolved in 40 mL of dichloromethane and acetone, respectively, under vigorous stirring. Then, proper amounts of TiO_2 or βCD-TiO_2 NPs (5% wt/wt) were homogenously dispersed in 10 mL of each solvent using ultrasonication for 15 min and then stirring for 30 min at room temperature. NPs suspensions were added dropwise to either PLA or CA solutions (7.5% wt/v) and then stirred for 2 h. These dispersions were poured onto Petri dishes to allow the solvents to evaporate in a hood at room temperature yielding films of uniform thickness (130 ± 10 μm). Then, the films thus obtained, bionanocomposites, were cut into 4 cm^2 square plates for biodegradation assays. For clarity, alphanumeric coding was used to identify each material prepared: a matrix identifier (CA or PLA) followed by two digits defining its content of additives. For instance, the system called PLA42 means a matrix made of PLA and containing both additives: TiO_2 at 4.2% and βCD at 0.8%. In this way, six different polymeric films (three for each matrix) were prepared according with the systems defined in Table 1.

Table 1
Identification of the polymeric films used in this study.

Polymeric matrix	System	TiO_2 content (%)	β-cyclodextrin content (%)
CA	CA00	0.0	0.0
	CA50	5.0	0.0
	CA42	4.2	0.8
PLA	PLA00	0.0	0.0
	PLA50	5.0	0.0
	PLA42	4.2	0.8

2.3. Biodegradation study

The aerobic biodegradation of PLA and CA polymers in aqueous medium was assessed in closed respirometers in accordance with standard procedure (ISO 14851:2020) for 100 days [35]. Secondary sludge (activated sludge) from a local wastewater treatment plant (Arazuri, Spain) was employed as microbial inoculum. The concentration of suspended solids in the inoculum was determined prior to the start of the assay, to estimate the optimal percentage of wastewater inoculum to be included in the respirometers. In the attempt to simulate a natural environment, an optimized test medium with high nutrient concentrations and buffering capacity was prepared as follows: 100 mL of solution A (37.5 g L^{-1} KH_2PO_4; 87.3 g L^{-1} Na_2HPO_4 $2H_2O$; 2.0 g L^{-1} NH_4Cl), 1 mL 22.5 g L^{-1} $MgSO_4$ $7H_2O$, 1 mL 36.4 g L^{-1} $CaCl_2$ $2H_2O$, 1 mL 0.25 g L^{-1} $FeCl_3$ $6H_2O$, 1 mL solution E (70 mg L^{-1} $ZnCl_2$; 100 mg L^{-1} $MnCl_2$ $4H_2O$; 6 mg L^{-1} H_3BO_3; 190 mg L^{-1} $CoCl_2$ $6H_2O$; 3 mg L^{-1} $CuCl_2$ $2H_2O$; 240 mg L^{-1} $NiCl_2$ $6H_2O$), water up to 1 L solution.

A battery of six batch 500-mL respirometers was installed, one for each sample: PLA, PLA 5% TiO_2, PLA 5% βCD-TiO_2, CA, CA 5% TiO_2, and CA 5% βCD-TiO_2 (see Supplementary information Figure S1). Each one was filled up with 150 mL solution, composed of 15% wastewater inoculum and 85% optimized test medium. In addition, 20 film samples (80 cm^2) were added to each flask as the only carbon source. Therefore, a head space of 350 mL of air was available in each system. The respirometers were hermetically closed and incubated under mild stirring (130 rpm) at 21 ºC for 100 days. The biodegradation of the samples was followed by measuring the daily BOD (Velp Scientifica, BOD sensor, Italy) and by mass loss of the testing films. Film samples were collected from the reactors every 5-days (taking advantage of the fact that the air was manually renewed in each respirometer), washed repeatedly with deionized water, and dried at 30 ºC for 24 h before characterization.

2.4. Characterization of nanocomposite films

The performance of PLA and CA nanocomposites over the 100-day biological degradation in sewage sludge was assessed by different techniques in order to see the role of TiO_2 NPs and βCD on their

biodegradability. PLA nanocomposites had entirely disappeared after 60-days testing, while CA films were not completely biodegraded even after 100 days. For that reason, the average testing times for each polymer were chosen as: initial time (0-day for both polymers), middle time (30-day for PLA, 50-day for CA) and end time (60-day for PLA, 100-day for CA). The experimental results were analyzed by Origin 2016 software.

2.4.1. Fourier transform infrared spectroscopy

FTIR analysis was performed under an attenuated total reflectance (ATR) method using a IRAffinity-1S Shimadzu FTIR spectrometer with a Golden Gate diamond ATR accessory. FTIR spectra of the polymeric samples were recorded every 5-days with a resolution of 4 cm^{-1} and 32 scans in a wavenumber range from 4000 to 600 cm^{-1}.

2.4.2. X-ray diffraction

The crystalline structure of the samples at the beginning, middle and end testing times was studied by X-ray diffraction (XRD) in a Bruker D8 Advance diffractometer employing Cu $K_{\alpha 1}$ radiation, from 5º to 60º (2θ), one second per step and step size of 0.03º. The calculations were performed using the diffractometer DIFFRAC.EVA software. The crystallinity index is calculated as the ratio of the area of crystalline peaks to the global area of crystalline plus amorphous peaks.

2.4.3. Thermogravimetry

TGA of the films was carried out every 15–20 days at a heating rate of 10 ºC min^{-1} under nitrogen atmosphere (TA instruments SDT650 Trios V5 software) between 25 and 1000 ºC using alumina crucibles.

2.4.4. Scanning electron microscopy

The microstructure of the nanocomposite films was observed in a Phenom ProX Desktop scanning electron microscope (SEM; Thermo Fisher Scientific, Waltham, MA, USA) operating at 5 keV, at the beginning, middle and end-times. Before analysis, the samples were covered with a thin gold layer using a Emitech K550 sputter coater. The image analysis was accomplished with ImageJ software.

3. Results And Discussion

3.1. Biodegradation study

Once the films (7.5% wt/v) were obtained, the biodegradability of the plain PLA and CA matrices was studied in comparison with their respective nanocomposites (with TiO_2 and βCD-TiO_2).

3.1.1. Biochemical oxygen demand

The results of BOD tests are presented in Fig. 1. It is noteworthy that oxygen consumption began almost immediately at the start of the test in the case of CA samples, with a very short acclimation period (2 days), whereas PLA films showed a first 5-day stage without oxygen depletion. This indicates that the amount of bacterial flora in the inoculum could be somewhat insufficient to meet the initial requirements for biodegradation, but also a need for acclimation to both substrates. It should also be noted that, except for a pre-filtration step, the inoculum was used as received, with no period of adaptation to CA and PLA substrates. Thus, with the inoculum used, the acclimation period for PLA as carbon source was clearly higher than that for CA. Moreover, for both PLA and CA nanocomposites, BOD measurements were markedly higher compared to those for the plain polymers. Likewise, a fairly linear trend was observed in the BOD curve for the plain films of CA and PLA, while the presence of the additives provided a more exponential growth to BOD profiles. This evidences that the additives improved the biodegradation of CA and PLA films. In the case of CA films, the addition of βCD (together with TiO_2) somewhat improved their biodegradability in the medium and long term. However, the opposite trend was found with those of PLA, where the presence of βCD appeared to delay degradation. Thereby, noticeable differences were observed with PLA films after 60-days incubation, reaching about 750 mg-O_2 L^{-1} for PLA00, 1100 mg-O_2 L^{-1} for PLA42, and 1600 mg-O_2 L^{-1} for PLA50 samples.

3.1.2. Mass loss

Mass losses measured during biodegradation assays with samples of nanocomposite and plain CA and PLA films are shown in Fig. 2. Mass loss of biopolymers is considered as the most basic and commonly used biodegradation index [36]. While CA films maintained the original square shape until the last testing day, PLA films began to crack and lose it after 30 days, so it was not possible to determine mass losses for the latter after that time. As expected, there is a close relationship between biodegradation time and mass loss of films; the longer the incubation time, the greater mass loss in samples. The biodegradation rate under respirometry conditions was significantly faster for CA and PLA nanocomposites than for the respective undoped materials. In the case of CA, the mass losses after 100 days of the nanocomposite films were substantially higher (49% and 53% for βCD-TiO_2 and TiO_2 nanocomposites, respectively) than that of the plain samples (39%). Similarly, higher mass losses were also obtained for PLA nanocomposites after 30 days (33% for TiO_2 and 20% βCD-TiO_2) than for the bare matrix (12%). As a reference, note that these results were quite comparable to those of CA samples after 30 days of incubation (29%, 36% and 19%, respectively). These results agree with those found with BOD assays (see Fig. 1). The modification of TiO_2 NPs with βCD is believed to make the resulting nanoparticles better integrated into the PLA matrix, strengthening its resistance to microbial activity. In this way, the higher the disruption of the polymer structure caused by NPs, the higher the rate of biodegradation of films. Comparing both polymers, the biodegradability of PLA systems under the microbial environment used was much better (they were completely disintegrated after 60 days; see Fig. 3) than that observed for CA composites.

3.2. Characterization of nanocomposite films

During the biodegradation assays, film samples were periodically collected from the respirometer flasks for physical and chemical characterization.

3.2.1. Physical appearance

The evolution of the physical appearance of the CA and PLA film probes throughout the trial is shown in Fig. 3. As observed, besides a natural twist in their original flatness due to the stirring shear forces, the undoped film probes did not exhibit any visible changes through the full test (100 days for CA and 60 days for PLA). However, alterations in the appearance of the doped composites were evident. On the one side, the CA42 and CA50 pieces became more twisted and shrunken, brittle and yellowish over time. On the other hand, the PLA nanocomposites, PLA42 and PLA50, rapidly began to crumble until complete disintegration. In fact, non-fragmented pieces of bare PLA were found even after 100 days of testing, which proves the effectiveness of PLA doping with TiO_2 and βCD-TiO_2 for its enhanced biodegradability.

3.2.2. FTIR analysis

The FTIR spectra of CA and PLA-based samples exposed to biodegradation tests are plotted in Figs. 4 and 5, respectively. The presence of the additives (TiO_2 and βCD) could not be evidenced by this technique since the Ti-O-O bond vibration appears at wavenumbers below 600 cm^{-1}, and the main peaks of βCD (present in low amount) were masked by the polymer bands.

The CA spectrum (Fig. 4 and S2) shows the main characteristic bands at approximately 3500 (O-H stretching vibration), 2930 (C-H stretching), 1740 (C = O stretching), 1640 (water O-H bending), 1370 (C-H symmetric bending), 1215 (C-O-C asymmetric stretching of acetate group), 1030 (C-O-C vibration in pyranoid ring), and 900 cm^{-1} (β-linked glucan structure) [37, 38]. The initial spectra of the films changed over time at a very different rate between samples. In all cases, the final spectrum (after 100 days testing) perfectly matched that of cellulose. However, the rate of deacetylation was much faster for the CA composites than for the bare CA. After the first 15 days of testing, the absorbance bands of carbonyl (1740 cm^{-1}), C-H (1370 cm^{-1}) and C-O-C (1215 cm^{-1}) groups in the CA50 and CA42 spectra had notably decreased, and they continued to decrease progressively until complete disappearance after 40 days. At the same time, a wide band appeared at 3300 cm^{-1} corresponding to the formation of O-H bonds. An abrupt drop in the vibration of the acetate groups was observed for the bare CA films after 50 days. Moreover, the theoretical mass loss for complete deacetylation is 37% [39], which agrees quite well with the data shown in Fig. 2. Thus, the CA nanocomposites had lost little more than 37% mass at day 50, while the bare CA polymer reached this value after 100 days. These outcomes show that biodegradation of CA was greatly accelerated by TiO_2 NPs. Nevertheless, βCD did not seem to have a notorious effect on this process, probably due to its presence in very low amount.

Different studies have demonstrated that the degradation mechanism of CA begins with the deacetylation of the material as the prior step to depolymerization of cellulose [40]. In addition, it has been reported that this initial step can occur by acetyl esterase enzymes or by chemical hydrolysis. Acetyl

esterases are common in many microorganisms and probably they were present in the mixed microbial culture of the wastewater inoculum [41]. Likewise, the testing duration was not sufficient for cellulose depolymerization, as FTIR spectra match with that of pure cellulose. Another study showed that cellulose fibers from toilet paper were biodegraded in activated sludge, albeit through a slow process and with a strong influence of temperature [42]. Therefore, probably if the present test had lasted longer, the CA films could have completely biodegraded.

FTIR spectra of PLA films were also obtained over the biodegradation time (Fig. 5). The characteristic peaks and bands of PLA polymer appear at: 2997 and 2947 cm^{-1} (corresponding to the C-H asymmetric and symmetric stretching vibrations, respectively); 1750 cm^{-1} (attributed to the C = O stretching); 1180 – 1000 cm^{-1} (related to C-O stretching vibrations); 1452 cm^{-1} (due to the -CH_3 group bending vibration); 1350–1380 cm^{-1} (represents C-H deformation bands); 870 cm^{-1} (from C-C stretching vibration). No significant chemical transformations were observed in the PLA probes throughout the biodegradation process, neither in terms of new peaks formation nor major shifts in the wavenumber of the characteristic PLA bands. Therefore, although the PLA pieces had collapsed after 60 days of testing, their chemical structure remained virtually unchanged from the initial one.

Nevertheless, the intensity of some peaks slightly varied throughout the test. The modifications were followed by calculating the height ratios of different signals with respect to the height of the peak at 1452 cm^{-1}, suitable standard for PLA (see Table S1 in Supplementary information). For the PLA50 and PLA42 nanocomposite films there is a decrease in the peak intensity of C = O (1750 cm^{-1}), CH-O (1180 cm^{-1}) and C-O-C (1080 cm^{-1}) over time, which indicates chain scissions of the structure [43]. These decreases in peak ratios were slightly more marked in the case of the unmodified TiO_2 composite (PLA50) than for the βCD-TiO_2 films (PLA42). In the case of bare PLA, smaller ratio changes were observed, with no clear trend. In any case, the addition of TiO_2 had a clearly positive effect on the biodegradation rate of PLA matrix.

3.2.3. X-ray diffraction analysis

The X-ray diffraction (XRD) patterns measured at the beginning of the biodegradation test (day 0), at the middle term (day 50 and 40 for CA and PLA, respectively), and at the end of the biodegradation test (day 100 for CA and day 60 for PLA) are depicted in Fig. 6. The presence of TiO_2 NPs in the bionanocomposites was well recognized. The crystallographic composition of TiO_2 is in good matching mainly with anatase phase (2θ = 25.2º, 37.1º, 48.1º), but also with rutile, showing a small diffraction peak at 2θ value of 27.4º. The main reflections of CA have been reported at 8º, 10º, 13º and 22º (2θ); the latest is known as Van der Waals halo and is present in most polymers as a result of the polymer chains packaging [44], as seen in all the diffractograms in Fig. 6. At the start of experiments, the computed crystallinity degree of CA was 39.5%, decreasing up to a 17.8% after 50-day testing. Moreover, as the biodegradation testing time increased, a clear shift toward higher 2θ was observed for the CA broad

pinnacle. This change on the 2θ angle was the main effect observed in all the CA samples and may be related with the polymeric degradation degree.

As observed in Fig. 6, the main diffraction peak of bare PLA (PLA00) appeared at 16.8º corresponding to (110)/(200) planes [45]. The intensity of this characteristic peak notably decreased with the incorporation of TiO_2 NPs, showing that PLA became more amorphous in the presence of titania. The XRD diffractograms of PLA composite including βCD (PLA42) also induced a partial loss of PLA crystallinity but to a lesser extent than unmodified TiO_2 composite (PLA50). This fact suggests that TiO_2 NPs act as disrupting agents, hindering the crystallization of PLA. Moreover, the polymer matrix of bare PLA films (PLA00) kept the crystalline structure after biodegradation tests (Table 2). However, substantial changes were appreciated for PLA42, which lost 20% crystallinity by the end of the test. In the case of PLA50, the main polymer peak almost had disappeared by day 30. While initially, the ratio between the intensity of the peaks at 25.2º (TiO_2) and 16.8º (PLA) was 3.20, after 60-days testing it became 6.83 (PLA 50 sample). The major BOD values and mass loss were also observed for this sample. In short, biodegradation rate of PLA films increased as polymer crystallinity decreased, which leads to conclude that there was a direct correlation between the resistance of the polymers towards biodegradation and their crystallinity grade, that is, the biodegradation rate increased as the polymer crystallinity decreased [46].

Table 2
Crystallinity degree of polylactic acid (PLA00), 5% TiO_2 PLA (PLA50), and 5% βCD-TiO_2 PLA (PLA42), at the beginning (0-day), middle (50-day for CA films, 30-day for PLA films) and end (100-day for CA; 60-day for PLA) of the biodegradation test.

	Crystallinity degree (%)		
Sample	0 days	30 days	60 days
PLA00	68.8	68.7	65.3
PLA50	88.4	85.8	66.1
PLA42	88.4	85.0	61.3

3.2.4. Thermogravimetric analysis

As an example, the thermograms obtained for CA and PLA-based samples before (day 0) and at the end of biodegradation tests (100 days for CA; 60 days for PLA) are shown in Fig. 7. Fig. S3 and S4 in Supplementary information collect the complete thermograms of CA and PLA-based films throughout the assay. Furthermore, for a better analysis of the thermal stability of CA and PLA films, some characteristic thermal values are listed in Tables 3 and 4, respectively. Titania NPs have high-thermal stability, and display a flat profile with no weight losses up to 1000 ºC [24]. As a result, the mass losses (Δm) (25-1000 ºC) obtained for the bare polymers are slightly higher than those of the corresponding composites.

TGA curves of CA samples show one main weight loss ranged from 250 ºC to 400 ºC due to the decomposition of the polymeric matrix. At this stage, cellulose can degrade through oxidation, decarboxylation and transglycosylation [47]. Some curves also display an initial drop below 150 ºC, attributed to water loss of samples. Fig. S5 in Supplementary information shows the first derivative of the normalized TGA profiles (DTG curves) of CA-based samples during the biodegradation assays. In the case of bare CA sample, the temperature at maximum decomposition speed (T_{DTG}) at day 0 appeared at 366 ºC. With the addition of 5% unmodified (CA50) and modified TiO_2 NPs (CA42), the temperature increased to 368 ºC and 369 ºC, respectively. This means that the inclusion of both type of NPs slightly reinforced the initial thermal stability of the CA matrix. As the testing time increased, T_{DTG} shifted to lower values, around 333 ºC after 100-days, similar for all the samples. However, while bare matrix (CA00) remained fairly stable up to day 50, the nanocomposites CA50 and CA42 lost great thermal resistance after the first 15 days (Table 3). The same phenomenon occurred with both initial (T_{onset}) and final degradation temperatures (T_{endset}), which decreased with biodegradation time and with TiO_2 NPs presence. At 348 ºC, the bare CA film began to lose mass, and ended at 381 ºC. After 100-days testing, these temperatures decreased to 309 ºC and 348 ºC, respectively. Also for CA nanocomposites, the temperatures decreased by more than 40 ºC between the beginning and the end of the biodegradation assays. In the case of 5% TiO_2 CA, T_{onset} decreased from 350 ºC to 308 ºC and T_{endset} from 383 ºC to 357 ºC. Finally, for 5% βCD-TiO_2, T_{onset} and T_{endset} values diminished in 77 ºC and 20 ºC, respectively (Table 3).

Table 3
Thermal properties of bare cellulose acetate (CA00), 5% TiO_2 (CA50) and 5% βCD-TiO_2 (CA42) nanocomposites throughout the 100-day biodegradation test.

CA	Time (days)	T_{onset} (ºC)	T_{DTG} (ºC)	T_{endset} (ºC)	Δm (%)
CA00	0	348	366	381	81.75
	15	323	357	377	84.37
	35	333	358	376	84.90
	50	332	357	375	78.73
	65	314	348	375	77.87
	85	307	335	356	69.49
	100	309	333	348	71.98
CA50	0	350	368	383	78.47
	15	320	347	373	80.16
	35	317	339	359	71.23
	50	319	338	356	66.38
	65	306	332	354	63.55
	85	303	333	356	62.77
	100	308	334	357	64.75
CA42	0	350	369	382	83.08
	15	311	340	367	78.22
	35	313	336	355	73.79
	50	308	336	356	68.86
	65	291	334	362	64.99
	85	275	327	358	63.25

TGA thermograms of PLA samples showed one weight loss corresponding to the thermal decomposition of the biopolymer (Fig. 7). Fig. S6 in the Supplementary information displays the DTG curves for PLA-based samples at different biodegradation times. The nearly identical initial (0-day) and final (60-day) peak temperatures (T_{DTG}) of the bare PLA sample, 364 ºC and 363 ºC, respectively, confirm the good thermal stability of the polymer throughout the assay. Likewise, PLA composites (PLA42 and PLA50) remained rather stable (T_{DTG}) until day 50 when a marked loss in thermal resistance occurred (366 ºC to

355 ºC for PLA50; and from 366 ºC to 359 ºC for PLA42 samples). Finally, the calculated enthalpy of thermal decomposition (ΔH_d) also decreased as test time increased (see Table 4).

The overall results exhibit an initial improvement in the thermal stability of the biopolymers with the addition of TiO_2 NPs, as reported by other authors [48]. In all cases, the higher the biodegradation time, the lower the thermal resistance of both polymers. This decrease was much more pronounced for PLA and CA nanocomposites than for the bare matrices. The nanocomposites were less resistant to the activity of the microbial consortium, and therefore their thermal properties substantially decreased. These results are in agreement with those obtained in subsection 3.2.3., suggesting that polymers with higher crystallinity are more resistant to enzymatic degradation, and therefore their thermal properties remain highly stable.

Table 4
Thermal properties of bare polylactic acid (PLA00), 5% TiO_2 (PLA50) and 5% βCD-TiO_2 (PLA42) throughout the 60-day biodegradation test.

PLA	Time (days)	T_{onset} (ºC)	T_{DTG} (ºC)	T_{endset} (ºC)	Δm (%)	ΔH_d (J/g)
PLA00	0	347	364	377	88.41	771.26
	15	348	366	379	95.03	840.05
	35	348	367	379	100.00	910.27
	50	346	365	379	90.92	792.25
	60	338	363	376	99.72	636.42
PLA50	0	351	366	377	86.21	820.00
	15	345	364	376	95.94	755.85
	35	310	338	353	92.14	316.89
	50	343	365	375	81.47	613.17
	60	322	355	368	87.32	292.96
PLA42	0	349	366	376	88.22	804.50
	15	333	359	371	94.99	559.73
	35	333	359	373	93.57	575.80
	50	326	358	369	83.90	445.71
	60	328	359	368	72.14	488.29

3.2.5. SEM analysis

Figure 8 and 9 show SEM micrographs on the surface morphology of PLA and CA-based films at the beginning and at the end of the biodegradation tests. Initially, all the samples exhibited a smooth surface,

and no TiO_2 agglomerates were observed, suggesting the well dispersion of the NPs in the polymeric matrices.

Attending to the microstructure of CA films, Fig. 8 shows large differences between samples. Bare CA films (CA00 system) suffered limited damage, presenting surface pitting after 100-days testing. On the other hand, SEM micrographs of unmodified TiO_2 composite (CA50) showed the greatest damage at the end of testing, revealing changes to a rougher surface and the formation of large holes (approximate diameter ranging from 50 to 120 μm). Finally, the nanocomposite containing CD-modified TiO_2 (CA42) showed voids and larger surface erosion than CA00.

As can be observed in Fig. 9, the appearance of bare PLA matrix did not show significant changes after 60-days, biodegradation, except for a few micro-size holes (ranging from 1 to 5 μm). However, the presence of TiO_2 and βCD-TiO_2 NPs clearly affected the morphology of the films, showing that PLA50 and PLA42 nanocomposites underwent substantial degradation. Thus, the films of both PLA nanocomposites appeared completely cracked and fragmented after 60-days of testing, showing large holes of up to 110 μm. The main difference between them was that nanocomposite containing βCD (PLA42) did not exhibit large fractures, while the unmodified TiO_2 composite (PLA50) presented a completely deteriorated appearance. SEM images of all the samples acquired at higher magnifications are collected in the Supplementary Information-Fig. S7 and S8 to better appreciate the morphology of the samples.

The overall results from SEM analyses show that the presence of TiO_2 clearly promoted the deterioration of both biopolymers by the microorganisms. Both types of NPs (βCD-modified and unmodified) played a role as a disrupting agent of the polymeric matrices, further enhancing the biodegradation rate of PLA and CA. Moreover, the presence of βCD seems to have a slightly protective effect on the polymers in comparison with the unmodified NPs. Previous studies have reported a stabilizing effect of the CDs on TiO_2 NPs [49], and this could improve its integration with the polymeric matrices. Comparing both biopolymers, PLA samples underwent greater damage in shorter times than CA. Under the biodegradation testing conditions, PLA films were easily degraded, while CA ones were more resistant to microbial attack. These findings support the results obtained by BOD analysis, mass loss, FTIR, XRD and thermogravimetry techniques, discussed in the previous sections.

4. Conclusions

In this work, CA and PLA composites including 5% TiO_2 and βCD-modified TiO_2 NPs were prepared and then exposed to an aerobic microbial consortium in order to study the effect of the added NPs on their biodegradability. The overall results show that, on the one hand, the addition of modified and unmodified TiO_2 NPs provided an initial reinforcement of the biopolymeric thermal properties. On the other hand, analyses on BOD, mass loss, FTIR, XRD, TGA and SEM lead to conclude that, TiO_2 NPs played a disrupting agent's role on the polymeric matrices, notably enhancing their biodegradation rates. Thus,

once the nanocomposite films shelf-life is ended, their disposal would be substantially faster and easier than that of the bare polymers. Furthermore, the presence of βCD seems to have a slightly protective effect on the polymers, attributed to its stabilizing effect on the TiO_2 NPs, that would improve its integration with the polymeric matrices. In addition, it has been observed that, polymers with higher crystallinity index are more resistant to biodegradation, and therefore their thermal properties remain highly stable over time. Finally, by comparing both polymers, PLA-based films were easily degraded before 100 days, whereas CA samples were more resistant to microbial attack and maintained their integrity after that period.

Declarations

Authors contribution: L.G-C: Conceptualization, Methodology, Formal analysis, Investigation and experiment performance, Writing-original draft preparation, Writing-review&editing. A.D: Conceptualization, Methodology, Analysis, Review&editing the manuscript. FJ.P: Conceptualization, Methodology, Analysis, Review&editing the manuscript. I.V: Conceptualization, Methodology, Analysis, Writing-review&editing, Project administration, Funding acquisition, Supervision.

Funding: The research was supported by Gobierno de Navarra (Project OPMATNAN PI017). L.G-C. gratefully acknowledges the Asociación de Amigos de la Universidad de Navarra for her doctoral grant.

Conflicts of Interest: The authors declare no conflicts of interest.

References

1. Morici E, Carroccio SC, Bruno E, Scarfato P, Filippone G, Dintcheva NT (2022) Recycled (Bio)Plastics and (Bio)Plastic Composites: A Trade Opportunity in a Green Future. Polymers (Basel) 14:2038 (1-24). https://doi.org/10.3390/polym14102038
2. Banerjee R, Ray SS (2022) Sustainability and Life Cycle Assessment of Thermoplastic Polymers for Packaging: A Review on Fundamental Principles and Applications. Macromol Mater Eng 307:1–22. https://doi.org/10.1002/mame.202100794
3. Nazrin A, Sapuan SM, Zuhri MYM, Ilyas RA, Syafiq R, Sherwani SFK (2020) Nanocellulose Reinforced Thermoplastic Starch (TPS), Polylactic Acid (PLA), and Polybutylene Succinate (PBS) for Food Packaging Applications. Front Chem 8:1–12. https://doi.org/10.3389/fchem.2020.00213
4. Gonçalves A, Helinando P, Oliveira P De (2022) Bio - based polymer films with potential for packaging applications : a systematic review of the main types tested on food. Polym Bull. https://doi.org/10.1007/s00289-022-04332-w
5. Siracusa V, Rosa MD (2018) Sustainable Packaging. In: Sustainable Food Systems from Agriculture to Industry: 275-307. https://doi.org/10.1016/B978-0-12-811935-8.00008-1
6. Arman Alim AA, Mohammad Shirajuddin SS, Anuar FH (2022) A Review of Nonbiodegradable and Biodegradable Composites for Food Packaging Application. J Chem 2022:1-27.

https://doi.org/10.1155/2022/7670819

7. Murariu M, Dubois P (2016) PLA composites: From production to properties. Adv Drug Deliv Rev 107:17–46. https://doi.org/10.1016/j.addr.2016.04.003
8. Di Maio L, Scarfato P, Avallone E, Galdi MR, Incarnato L (2014) Preparation and characterization of biodegradable active PLA film for food packaging. AIP Conf Proc 1593:338–341. https://doi.org/10.1063/1.4873795
9. Marano S, Laudadio E, Minnelli C, Stipa P (2022) Tailoring the Barrier Properties of PLA: A State-of-the-Art Review for Food Packaging Applications. Polymers (Basel) 14:1-44. https://doi.org/10.3390/polym14081626
10. Zhang M, Biesold GM, Choi W, Yu J, Deng Y, Silvestre C, Lin Z (2022) Recent advances in polymers and polymer composites for food packaging. Mater Today 53:134-161. https://doi.org/10.1016/j.mattod.2022.01.022
11. Lagaron JM (2011) Polylactic acid (PLA) for food packaging applications. In: José-María Lagarón (ed) Multifunctional and Nanoreinforced Polymers for Food Packaging, 1st Editio. pp 485–497
12. Assis RQ, Rios PDA, Rios A de O, Olivera FC (2020) Biodegradable packaging of cellulose acetate incorporated with norbixin, lycopene or zeaxanthin. Ind Crops Prod 147:112212 (1-11). https://doi.org/10.1016/j.indcrop.2020.112212
13. Claro PIC, Neto ARS, Bibbo ACC, Mattoso LHC, Bastos MSR, Marconcini JM (2016) Biodegradable Blends with Potential Use in Packaging: A Comparison of PLA/Chitosan and PLA/Cellulose Acetate Films. J Polym Environ 24:363–371. https://doi.org/10.1007/s10924-016-0785-4
14. Mesgari M, Aalami AH, Sahebkar A (2021) Antimicrobial activities of chitosan/titanium dioxide composites as a biological nanolayer for food preservation: A review. Int J Biol Macromol 176:530–539. https://doi.org/10.1016/j.ijbiomac.2021.02.099
15. U.S. Food and Drug Administration (FDA) (2020) CFR - Code of Federal Regulations Title 21
16. Garcia C V., Shin GH, Kim JT (2018) Metal oxide-based nanocomposites in food packaging: Applications, migration, and regulations. Trends Food Sci Technol 82:21–31. https://doi.org/10.1016/j.tifs.2018.09.021
17. Zhang W, Rhim JW (2022) Titanium dioxide (TiO2) for the manufacture of multifunctional active food packaging films. Food Packag Shelf Life 31:100806 (1-12). https://doi.org/10.1016/j.fpsl.2021.100806
18. Mulla MZ, Rahman MRT, Marcos B, Tiwari B, Pathania S (2021) Poly lactic acid (PLA) nanocomposites: Effect of inorganic nanoparticles reinforcement on its performance and food packaging applications. Molecules 26:1-22. https://doi.org/10.3390/molecules26071967
19. Zhang H, Jintao H, Li Y, Rongyuan C, Wei Z, Xiangkun L, Jinping Q (2015) Preparation, characterization and properties of PLA/TiO_2 nanocomposites based on novel vane extruder. RSC Adv 5:4639–4647

20. Mathur V (2018) Dynamic mechanical analysis of PVC / TiO_2 nanocomposites. Adv Compos Hybrid Mater 1:741–747. https://doi.org/10.1007/s42114-018-0051-4
21. Goñi-Ciaurriz L, Vélaz I (2022) Antibacterial and degradable properties of β -cyclodextrin-TiO_2 cellulose acetate and polylactic acid bionanocomposites for food packaging. Int J Biol Macromol 216:347–360. https://doi.org/10.1016/j.ijbiomac.2022.06.202
22. Gu XY, Hu LM, Fu ZA, Wang HT, Li YJ (2021) Reactive TiO_2 Nanoparticles Compatibilized PLLA/PBSU Blends: Fully Biodegradable Polymer Composites with Improved Physical, Antibacterial and Degradable Properties. Chinese J Polym Sci 39:1645–1656. https://doi.org/10.1007/s10118-021-2632-x
23. Jang J, Lee HS, Lyoo WS (2007) Effect of UV irradiation on cellulase degradation of cellulose acetate containing TiO_2. Fibers Polym 8:19–24. https://doi.org/10.1007/BF02908155
24. Goñi-ciaurriz L, Senosiain-nicolay M, Vélaz I (2021) Aging studies on food packaging films containing β-cy-clodextrin-grafted tio2 nanoparticles. Int J Mol Sci 22:1–13. https://doi.org/10.3390/ijms22052257
25. Goñi-Ciaurriz L, González-Gaitano G, Vélaz I (2020) Cyclodextrin-grafted nanoparticles as food preservative carriers. Int J Pharm 588:119664 (1-8). https://doi.org/10.1016/j.ijpharm.2020.119664
26. Davis ME, Brewster ME (2004) Cyclodextrin-based pharmaceutics: Past, present and future. Nat Rev Drug Discov 3:1023–1035. https://doi.org/10.1038/nrd1576
27. Velázquez-Contreras F, Zamora-Ledezma C, López-González I, Meseguer-Olmo L, Núñez-Delicado E, Gabaldón JA (2022) Cyclodextrins in Polymer-Based Active Food Packaging : A Fresh Look at Nontoxic, Biodegradable, and Sustainable Technology Trends. Polymers (Basel) 14:1–29. https://doi.org/10.3390/polym14010104
28. Liu Y, Sameen DE, Ahmed S, Wang Y, Lu R, Dai J, Li S, Qin W (2022) Recent advances in cyclodextrin-based films for food packaging. Food Chem 370:131026 (1-13). https://doi.org/10.1016/j.foodchem.2021.131026
29. Verstichel S, De Wilde B, Fenyvesi E, Szejtli J (2004) Investigation of the Aerobic Biodegradability. J Polym Environ 12:47–55. https://doi.org/10.1023/B:JOOE.0000010050.52967.94
30. Szente L, Fenyvesi É (2018) Cyclodextrin-enabled polymer composites for packaging. Molecules 23:1–18. https://doi.org/10.3390/molecules23071556
31. Kumar S, Kumar M, Kumar V, Sarsaiya S (2022) A comprehensive review on recent advancements in biodegradation and sustainable management of biopolymers . Environ Pollut 307:119600 (1-20). https://doi.org/10.1016/j.envpol.2022.119600
32. Kliem S, Kreutzbruck M, Bonten C (2020) Review on the Biological Degradation of Polymers in Various Environments. Materials (Basel) 13:4586 (1–18)
33. Jouanneau S, Recoules L, Durand MJ, Boukabache A, Picot V, Primault Y, Lakel A, Sengelin M, Barillon B, Thouand G (2014) Methods for assessing biochemical oxygen demand (BOD): A review. Water Res 49:62–82. https://doi.org/10.1016/j.watres.2013.10.066

34. Pagga U (1997) Testing biodegradability with standardized methods. Chemosphere 35:2953–2972. https://doi.org/10.1016/S0045-6535(97)00262-2
35. International Organization for Standardization (2020) UNE-EN ISO 14851: Determination of the ultimate aerobic biodegradability of plastic materials in an aqueous medium - Method by measuring the oxygen demand in a closed respirometer.
36. Pires A, Gomes V, Souza L, Fuciños P, Pastrana L, Lu A (2022) Methodologies to Assess the Biodegradability of Bio-Based Polymers — Current Knowledge and Existing Gaps. Polymers 14:1359 (1-24). https://doi.org/10.3390/polym14071359
37. Hwan J, Kwak LS (2022) Switchable degradation of cellulose acetate composite by seawater-activated TiO_2 photocatalyst. Cellulose 29:1501–1508. https://doi.org/10.1007/s10570-021-04381-w
38. Kaur H, Bulasara VK, Gupta RK (2018) Influence of pH and temperature of dip-coating solution on the properties of cellulose acetate-ceramic composite membrane for ultra filtration. Carbohydr Polym 195:613–621. https://doi.org/10.1016/j.carbpol.2018.04.121
39. Yadav N, Hakkarainen M (2022) Degradation of Cellulose Acetate in Simulated Aqueous Environments : One - Year Study. Macromol Mater Eng 307:2100951 (1–9). https://doi.org/10.1002/mame.202100951
40. Puls J, Wilson SA, Hölter D (2011) Degradation of Cellulose Acetate-Based Materials: A Review. J Polym Environ 19:152–165. https://doi.org/10.1007/s10924-010-0258-0
41. Boczar BA, Begley WM, Larson RJ, Boczar BA, Begley WM, Larson RJ (1992) Characterization of enzyme activity in activated sludge using rapid analyses for specific hydrolases. Water Environ Res 64:792–797.
42. Ruiken CJ, Breuer G, Klaversma E, Santiago T, van Loosdrecht MCM (2013) Sieving wastewater - Cellulose recovery, economic and energy evaluation. Water Res 47:43–48. https://doi.org/10.1016/j.watres.2012.08.023
43. Nitin A, Kachenchart B, Wongthanaroj A (2022) Rapid biodegradation of high molecular weight semi-crystalline polylactic acid at ambient temperature via enzymatic and alkaline hydrolysis by a defined bacterial consortium. Polym Degrad Stab 202:110051 (1-15). https://doi.org/10.1016/j.polymdegradstab.2022.110051
44. Meireles S, Rodrigues G, Fernandes M, Jr F, Alves D, Maria R, Assunção N, Angélica E, Ribeiro M, Poletto P, Zeni M (2010) Characterization of asymmetric membranes of cellulose acetate from biomass : Newspaper and mango seed. Carbohydr Polym 80:954–961. https://doi.org/10.1016/j.carbpol.2010.01.012
45. Zhang J, Duan Y, Sato H, Tsuji H, Noda I, Yan S, Ozaki Y (2005) Crystal Modifications and Thermal Behavior of Poly (L -lactic acid) Revealed by Infrared Spectroscopy. Macromolecules 38:8012–8021. https://doi.org/10.1021/ma051232r
46. Roijen EC Van, Miller SA (2022) A review of bioplastics at end-of-life : Linking experimental biodegradation studies and life cycle impact assessments. Resour Conserv Recycl 181:106236 (1-

16). https://doi.org/10.1016/j.resconrec.2022.106236

47. Dufresne A (2013) Nanocellulose: A new ageless bionanomaterial. Mater Today 16:220–227. https://doi.org/10.1016/j.mattod.2013.06.004
48. Mahmoudi E (2020) Improvement Thermomechanical Properties of Polylactic Acid via Titania Nanofillers Reinforcement. J Adv Res Fluid Mech Therm Sci 1:97–111. https:/doi.org/10.37934/arfmts.70.1.97111
49. Agócs TZ, Puskás I, Varga E, Molnár M (2016) Stabilization of nanosized titanium dioxide by cyclodextrin polymers and its photocatalytic effect on the degradation of wastewater pollutants Stabilization of nanosized titanium dioxide by cyclodextrin polymers and its photocatalytic effect on the degrad. J Org Chem 12:2873–2882. https://doi.org/10.3762/bjoc.12.286

Figures

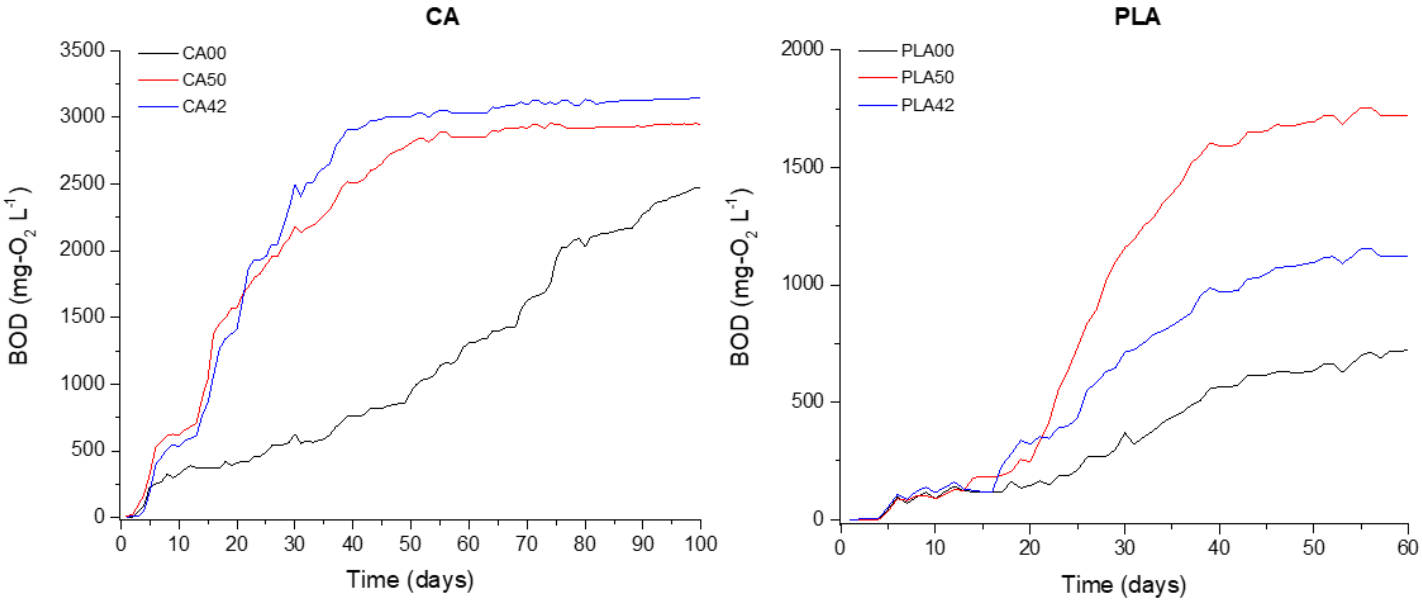

Figure 1

Biochemical oxygen demand (BOD) profiles in the biodegradation assays: (a) cellulose acetate (CA00), CA 5% TiO2 (CA50) and CA 5% βCD-TiO2 (CA42); (b) polylactic acid (PLA00), PLA 5% TiO2(PLA50) and PLA 5% βCD-TiO2 (PLA42).

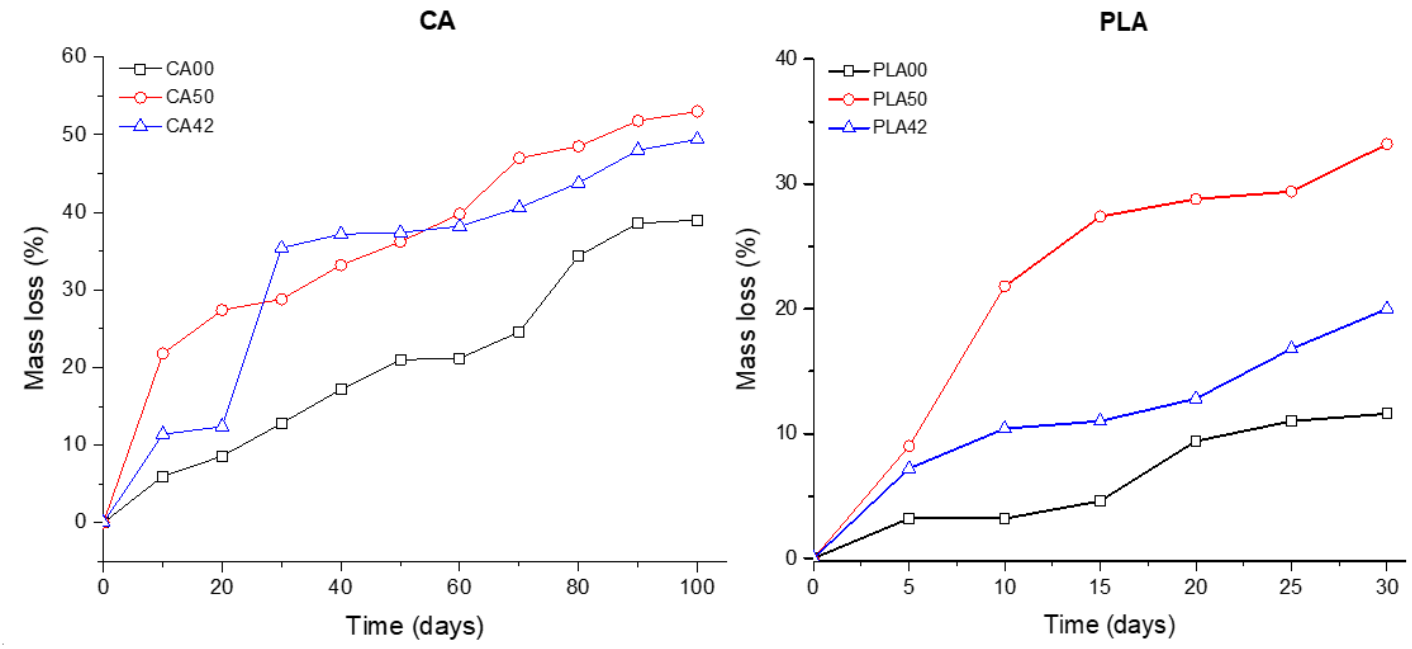

Figure 2

Evolution of mass loss of cellulose acetate (CA00), CA 5% TiO2(CA50) and CA 5% βCD-TiO2(CA42); polylactic acid (PLA00), PLA 5% TiO2 (PLA50) and PLA 5% βCD-TiO2(PLA42) films through the biodegradation tests.

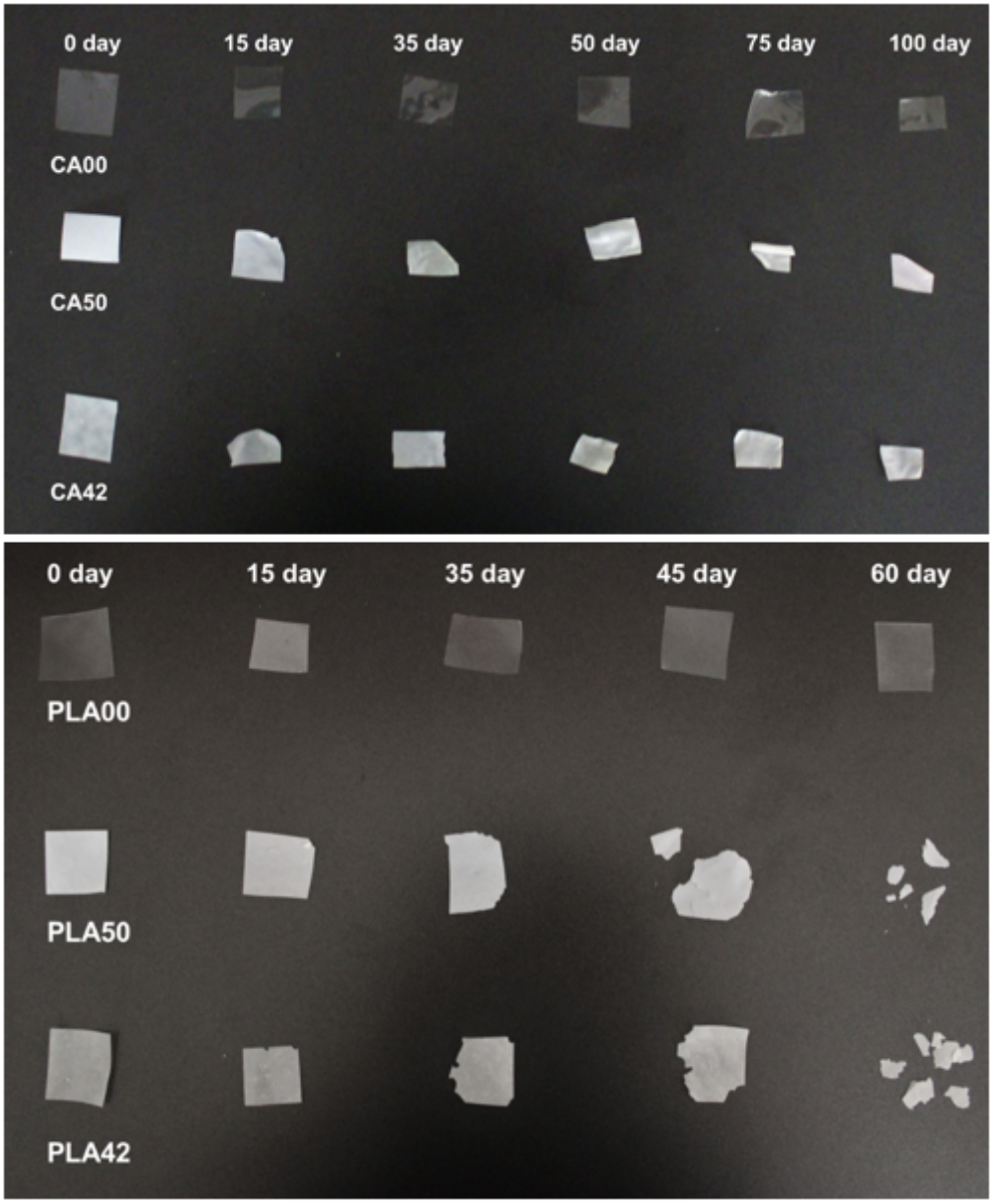

Figure 3

Photographs of cellulose acetate (CA00), CA 5% TiO2 (CA50), and CA 5% βCDTiO2 (CA42); polylactic acid (PLA00), PLA 5% TiO2 (PLA50), and PLA 5% βCDTiO2(PLA42), throughout the biodegradation test.

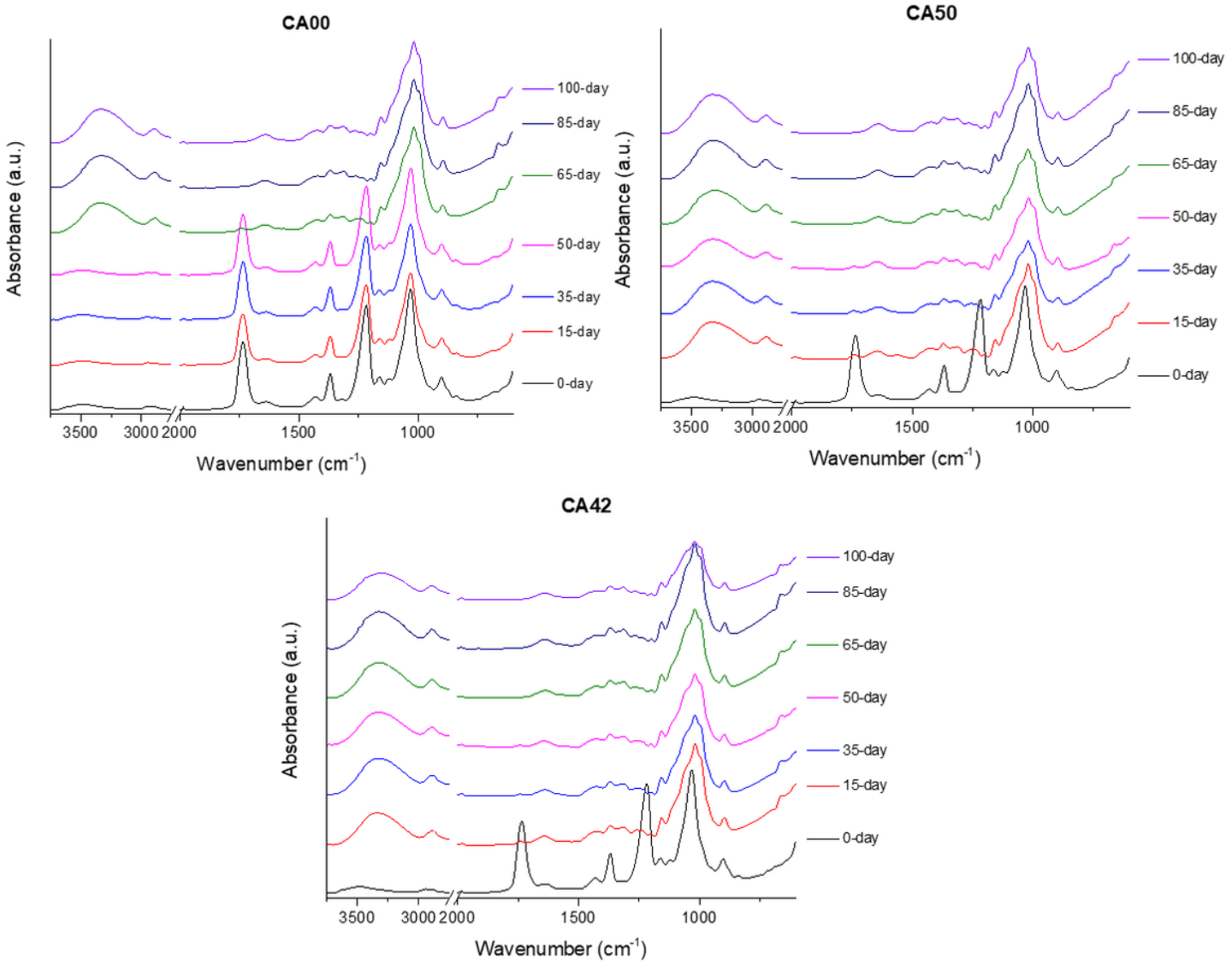

Figure 4

FTIR spectra of bare cellulose acetate (CA00) and their 5% TiO2 (CA50) and 5% βCD-TiO2(CA42) nanocomposites throughout the biodegradation test.

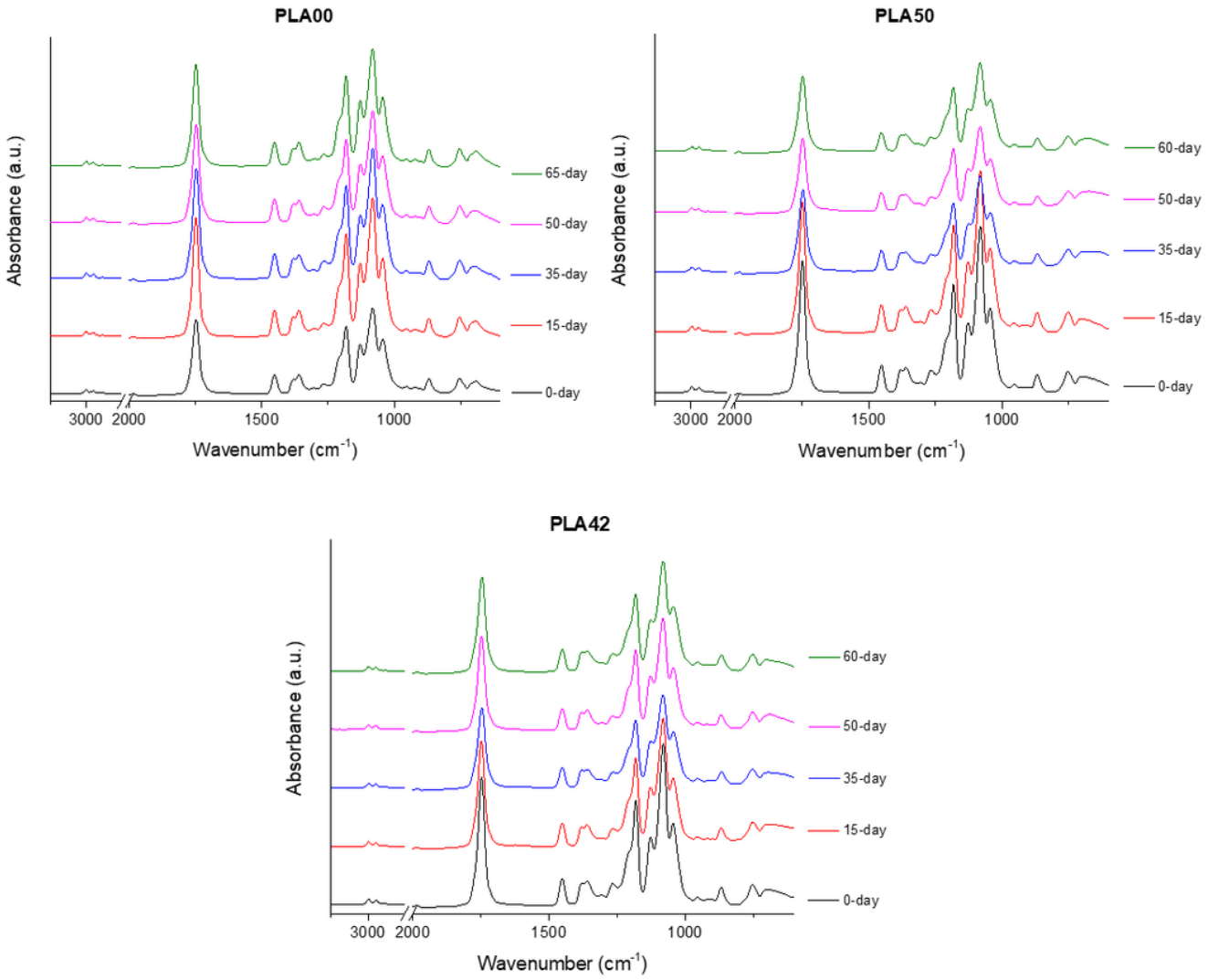

Figure 5

FTIR spectra of bare polylactic acid (PLA00) and their 5% TiO2 (PLA50) and 5% βCD-TiO2(PLA42) nanocomposites throughout the biodegradation test.

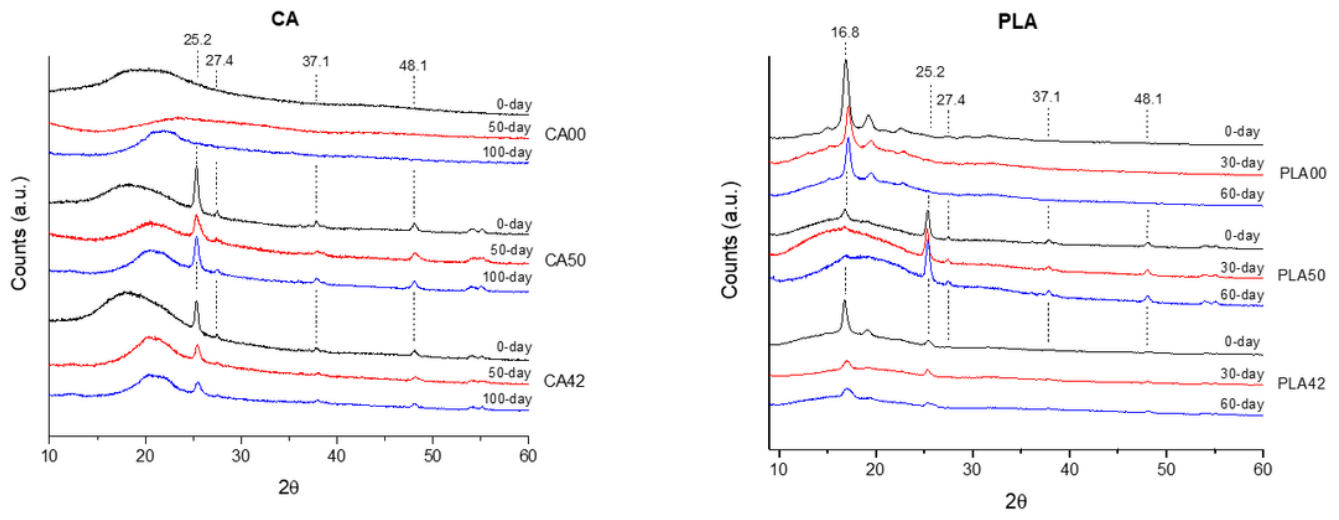

Figure 6

X-ray diffraction (XRD) patterns of cellulose acetate (CA00), CA 5% TiO2 (CA50) and CA 5% βCD-TiO2(CA42); polylactic acid (PLA00), PLA 5% TiO2 (PLA50) and PLA 5% βCD-TiO2(PLA42) films at the beginning (0-day), middle (50-day for CA films, 30-day for PLA films) and end (100-day for CA; 60-day for PLA) of the biodegradation test.

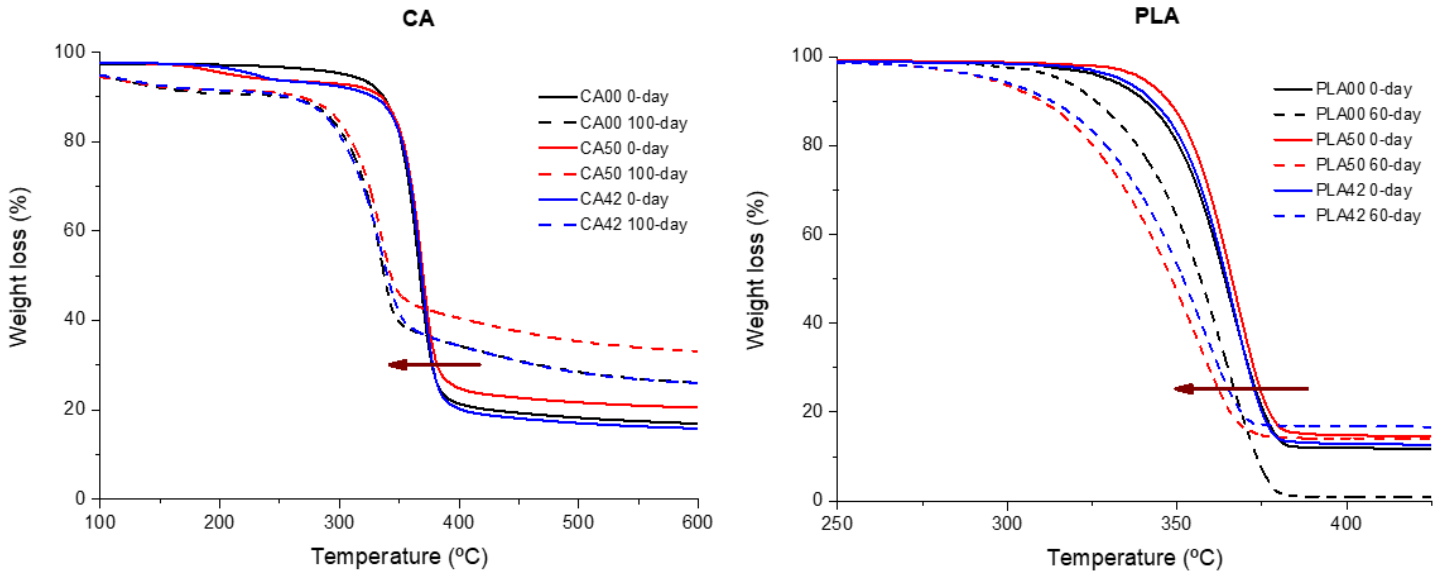

Figure 7

TGA thermograms of cellulose acetate (CA00), CA 5% TiO2 (CA50) and CA 5% βCD-TiO2(CA42); polylactic acid (PLA00), PLA 5% TiO2 (PLA50) and PLA 5% βCD-TiO2(PLA42) at the beginning (0-day) and end (100-day for CA; 60-day for PLA) of the biodegradation test.

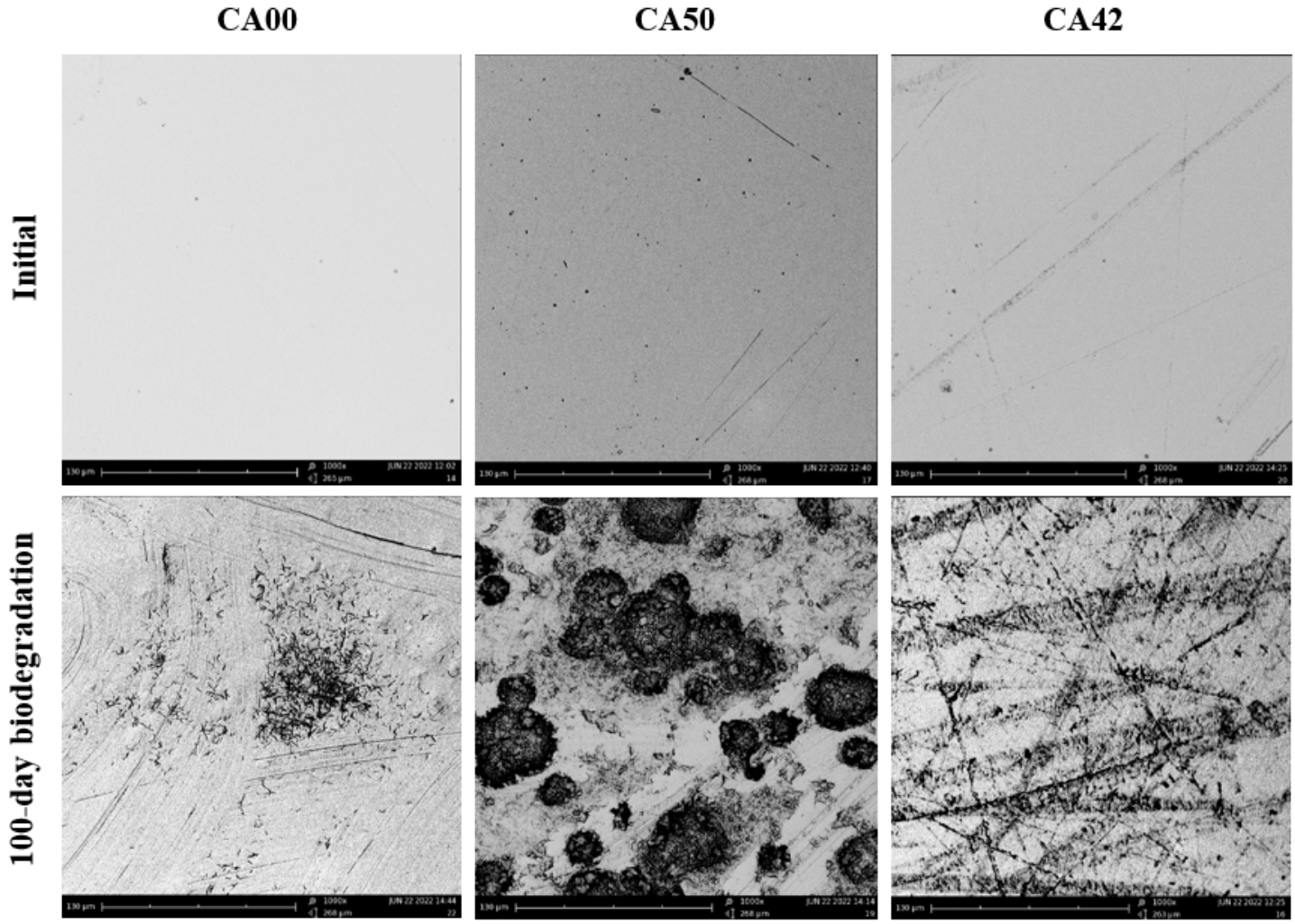

Figure 8

Scanning electron microscopy (SEM) images (1000x) corresponding to cellulose acetate (CA00), CA 5% TiO2 (CA50) and CA 5% βCD-TiO2(CA42) films before and after exposure to 100-day biodegradation test.

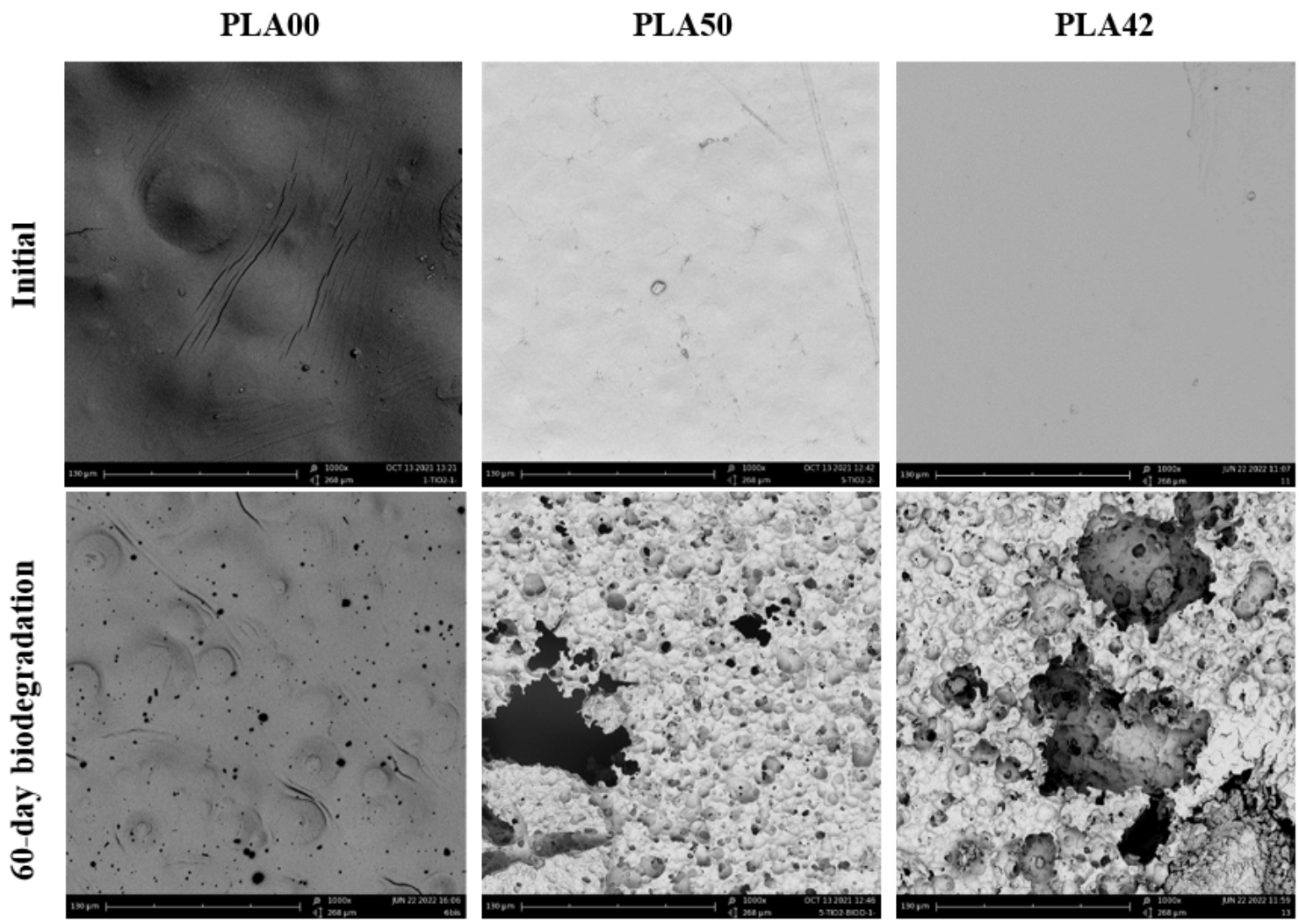

Figure 9

Scanning electron microscopy (SEM) images (1000x) corresponding to polylactic acid (PLA00), PLA 5% TiO2 (PLA50) and PLA 5% βCD-TiO2(PLA42) films before and after exposure to 60-day biodegradation test.

Supplementary Files

This is a list of supplementary files associated with this preprint. Click to download.

- Graphicalabstract.pdf
- Supplementaryinformation.docx